
On Lottery Tickets and Minimal Task Representations in Deep Reinforcement Learning

Marc Vischer *
 Technical University Berlin
 vischer@campus.tu-berlin.de

Robert Tjarko Lange *
 Technical University Berlin
 robert.t.lange@tu-berlin.de

Henning Sprekeler
 Technical University Berlin
 henning.sprekeler@tu-berlin.de

Abstract

The lottery ticket hypothesis questions the role of overparameterization in supervised deep learning. But how is the performance of winning lottery tickets affected by the distributional shift inherent to reinforcement learning problems? In this work, we address this question by comparing sparse agents who have to address the non-stationarity of the exploration-exploitation problem with supervised agents trained to imitate an expert. We show that feed-forward networks trained via reinforcement learning and imitation learning can be pruned to the same level of sparsity, suggesting that the distributional shift has a limited impact on the size of winning tickets. Using a set of carefully designed baseline conditions, we find that the majority of the lottery ticket effect in both learning paradigms can be attributed to the identified mask rather than the weight initialization. The input layer mask selectively prunes entire input dimensions that turn out to be irrelevant for the task at hand. At a moderate level of sparsity the mask identified by iterative magnitude pruning yields minimal task-relevant representations, i.e., an interpretable inductive bias. Finally, we propose a simple initialization rescaling which promotes the robust identification of sparse task representations in low-dimensional control tasks.

1 Introduction

Recent research on the lottery ticket hypothesis (LTH, Frankle and Carbin, 2019; Frankle et al., 2019) in deep learning has demonstrated the existence of very sparse neural networks that train to performance levels comparable to those of their dense counterparts. These results challenge the role of overparameterization in supervised learning and provide a new perspective on the emergence of stable learning dynamics (Frankle et al., 2020a,b). Recently these results have been extended to various domains beyond supervised image classification. These include self-supervised learning (Chen et al., 2020a), natural language processing (Yu et al., 2019; Chen et al., 2020b) and semantic segmentation (Girish et al., 2020). But how does the lottery ticket phenomenon transfer to reinforcement learning agents? One key challenge may be the inherent non-stationarity of the optimization problem in deep reinforcement learning (DRL): The data-generation process is not static, but depends on the changing state of the neural network. Furthermore, a weight may serve different roles at different stages of learning (e.g. during exploration and exploitation). It is not obvious how a simple weight

*These two authors contributed equally. Robert Tjarko Lange is the corresponding author.

magnitude-based pruning heuristic acting on a well-performing policy shapes the learning process of the agent. In this work, we therefore investigate winning tickets in reinforcement learning and their underlying contributing factors. We compare supervised imitation learning with DRL, putting a special emphasis on the resulting input representations used for prediction and control. Thereby, we connect the statistical perspective of sparse structure discovery (e.g. Hastie et al., 2019) with the iterative magnitude pruning (IMP, Han et al., 2015) procedure in the context of Markov decision processes (MDPs). The contributions of this work are summarized as follows:

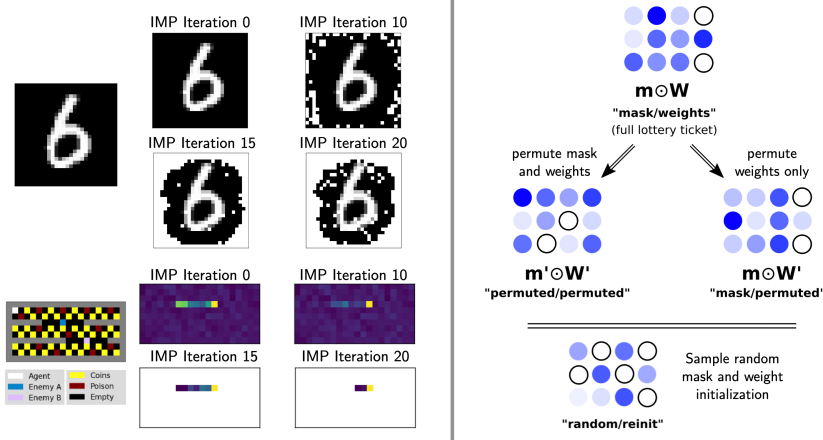


Figure 1: Representation compression and a schematic of the set of disentangling baselines. **Left.** IMP successively prunes task-irrelevant outer rim pixels in a MNIST digit-classification task. A similar representation compression emerges for an IMP-masked agent solving a visual navigation task in DRL. The channel that encodes the patrolling enemy is pruned up to the point where only potential enemy locations are considered. **Right.** To disentangle the contributions of mask, initialization and layer-wise pruning ratio to the winning lottery ticket (corresponding to condition *mask/weights*), we compare three baselines: After each IMP iteration, we permute either only the remaining initial weights (*mask/permuted*) or also the sparsity mask (*permuted/permuted*). The third baseline is created by randomly sampling a sparse mask and random re-initialization of the weights (*random/re-init*). It no longer preserves the layer-wise pruning ratio of the lottery ticket.

1. We show that winning tickets exist in both high-dimensional visual and classic control tasks. A positive lottery ticket effect is robustly observed for both off-policy DRL algorithms, including Deep-Q-Networks (DQN, Mnih et al., 2015) and on-policy policy-gradient methods (PPO, Schulman et al., 2017), providing evidence that the lottery ticket effect is a universal phenomenon across optimization formulations in DRL.
2. By comparing reinforcement learning to supervised policy distillation, we show that networks can be pruned to similar sparsity levels before performance starts to degrade, indicating that the covariate shift does not require larger winning tickets (section 3.1).
3. We show that the suggestion of larger networks providing a combinatorially larger number of candidate tickets does not hold for the tasks we tested. Smaller networks can in fact be pruned more strongly in terms of the absolute number of remaining weights.
4. By introducing a set of lottery ticket baselines (section 3; figure 1, right column), we disentangle the contributions of the mask, weight initialization and layer-wise pruning ratio. We demonstrate that the mask explains most of the ticket effect for MLP-based agents, whereas the associated weight initialization is less important (section 3.2). For more challenging environments and CNN-based agents the weight initialization contributes more.
5. By visualizing the sparsified weights for each layer, we find that early network layers are pruned more. Entire input dimensions can be rendered invisible to MLP-based agents by the pruning procedure. By this mechanism, IMP compresses the input representation of the MDP (e.g. figure 1, left column, bottom row) and reveals a minimal task representation for the underlying control problems (section 4).

6. The IMP input layer mask not only eliminates obviously redundant dimensions, but also identifies complex relationships between input features and the task of the agent (section 4.1), e.g. the proximity of an enemy or the speed of an approaching object. We show that the input masking can be transferred to train dense agents with sparse inputs at lower costs.
7. We show that the weight initialization scheme is crucial for discovering minimal representations. Depending on the input size of different layers of the network, global magnitude-based pruning can introduce a strong layer-specific pruning bias. We compare initializations and show that a suitable initialization scheme enables the removal of task-irrelevant dimensions (section 4.2).

2 Background and Related Work

Iterative Magnitude Pruning. We use the iterative pruning procedure outlined in Frankle and Carbin (2019) to identify winning tickets. We train DRL agents for a previously calibrated number of transitions and track the best performing network checkpoint throughout. Performance is measured by the average return on a set of evaluation episodes. Afterwards, we prune 20% of the weights with smallest magnitude globally (across all layers). The remaining weights are reset to their initial values and we iterate this procedure (train \rightarrow prune \rightarrow reset).² The *lottery ticket effect* refers to the performance gap between the sparse network obtained via IMP and a randomly initialized network with sparsity-matched random pruning mask.

Lottery Tickets in Deep Reinforcement Learning. Yu et al. (2019) previously demonstrated the existence of tickets in DRL that outperform parameter-matched random initializations. They obtained tickets for a distributed on-policy actor-critic agent on a subset of environments in the ALE benchmark (Bellemare et al., 2013) as well as a set of control tasks. While they provide empirical evidence for the existence of lottery tickets in DRL, they did not investigate the underlying mechanisms. Here, we try to unravel these mechanisms. To this end, we focus on a small set of environments and provide a detailed comparison between supervised policy distillation and on-/off-policy Deep RL with a set of carefully designed ticket baselines. We analyze the resulting masked representations that the agent learns to act upon and the impact of specific weight initializations on the resulting sparse networks.

Lottery Tickets with Non-Stationary Data Distributions. Desai et al. (2019) investigated whether trained lottery tickets overfit the training data distribution under which they were obtained. Using transfer learning tasks on natural language data, they showed that lottery tickets provide general inductive biases. Similar ticket transfer results were reported by Morcos et al. (2019) and Mehta (2019) in the context of optimizers and vision datasets. Unlike our work, these studies do not investigate within-training covariate shift, but instead focus on transferring ticket initializations after a full IMP run. Chen et al. (2021), on the other hand, investigate the ticket phenomenon in the context of lifelong learning and class-incremental image classification. They propose new pruning strategies to overcome the sequential nature of tasks and need for increased model capacity. Compared to the DRL setting, the covariate shift is here determined by the curriculum schedule of tasks and not the exploration behaviour of the network-parameterized agent.

On-Policy and Off-Policy Deep Reinforcement Learning. In our off-policy DRL experiments, we train Deep-Q-Networks (DQN, Mnih et al., 2015) with double Q-learning loss (Van Hasselt et al., 2016) and prioritized experience replay (Schaul et al., 2015). For illustrative purposes, we first train DQN agents on a visual navigation task, in which an agent has to collect coins in a maze while avoiding poison and two patrollers that are moving in restricted parts of the maze (figure 1, left column, bottom row; SI A). We scale our results to the MinAtar environments (Young and Tian, 2019), which capture many core features of the ALE benchmark and have been shown to reproduce their qualitative insights into value-based DRL methods (Obando-Ceron and Castro, 2020). As a representative on-policy algorithm, we chose Proximal Policy Optimization (PPO, Schulman et al., 2017). PPO is a baseline-corrected policy gradient algorithm which uses a clipping strategy to approximate a computationally expensive trust-region optimization method. The PPO agents are trained to solve the classic four dimensional cart-pole and six dimensional acrobot swing-up control

²In supervised learning, the pruning mask is often constructed based on an early stopping criterion and the final network. We instead track the best performing agent. Thereby, we reduce noise introduced by unstable learning dynamics and exploit that the agent is trained and evaluated on the same environment. We found that late rewinding to a later checkpoint (Frankle et al., 2019) is not necessary for obtaining tickets (SI figure 11).

tasks. For all experiments, we train feedforward value estimators and policies. All hyperparameters and the training amount were calibrated for their respective environments (SI B).

Supervised Imitation Learning via Policy Distillation. While most supervised learning relies on a stationary data distribution provided by a static dataset, reinforcement learning agents have to acquire their training data in an action-perception loop. Since the agent’s behavioural policy is learned over time, the data distribution used in optimization undergoes covariate shift. To study how the covariate shift influences winning tickets, we mimic the supervised learning case by training agents via supervised policy distillation (Rusu et al., 2015; Schmitt et al., 2018). We roll out a pre-trained expert policy and train the student agent by minimizing either the mean-squared error between the student’s and teacher’s Q -value predictions (off-policy) or the cross-entropy between the student’s and teacher’s softmax policies (on-policy).

3 Disentangling Contributions via Fine-Grained Baselines

There are two contributing factors to the lottery ticket effect: The IMP-identified binary mask and the preserved initialized weights that remain after pruning (*mask/weights*). We aim to disentangle the contributions by introducing a set of counterfactual baselines, which modify the original IMP procedure (figure 1, right column; table 1). A first baseline estimates how much of the performance of the ticket can be attributed to the initial weights, by means of a layer-specific permutation of the weights that remain after masking (*mask/permuted*). A second, weaker baseline estimates the contribution of the mask, by also permuting the layer-specific masks (*permuted/permuted*). Finally, we consider the standard *random/re-init* baseline, which samples random binary masks – discarding layer-specific pruning ratios – and re-initializes all weights at each IMP iteration. Throughout the next sections we use these baselines to analyze and compare the factors that give rise to the lottery ticket effect in different control settings.

Examined Sparsity-Generating IMP Variants			
	Retain weights	Retain mask	Retain layer pruning ratio
<i>mask/weights</i>	✓	✓	✓
<i>mask/permuted</i>	✗	✓	✓
<i>permuted/permuted</i>	✗	✗	✓
<i>random/re-init</i>	✗	✗	✗

Table 1: Proposed Baselines for Disentangling Ticket Contributions

3.1 Disentangling Ticket Contributions in Supervised Policy Distillation

Does the covariate shift in DRL affect the existence and nature of lottery tickets? Weights pruned for their small magnitude at the end of the learning process might be needed at earlier stages, e.g., during exploration. If this were the case, the performance of the ticket in DRL should degrade for lower levels of sparsity than in a corresponding supervised task. To investigate this question, we turn to a policy distillation setting, in which a randomly initialized student agent is trained to directly match the value estimates (DQN expert) or imitate the stochastic policy (PPO expert) of a dense pre-trained expert. By collecting transitions based on the static behavioral policy of the expert, we avoid the need for exploration and the effect of an otherwise non-stationary data distribution. We trained the agent on the supervised learning signal provided by the expert and applied magnitude pruning after each training run iteration. The procedure is repeated for all previously introduced baselines and multiple independent runs. For both the value estimate-distilled maze agents and the policy-distilled cart-pole agents we find that the RL setting and the supervision setting start to degrade in performance at similar sparsity levels (figure 2, left column). This suggests that for the considered tasks the non-stationarity introduced by the action-perception loop does not impede the minimal size of the ticket.

To disentangle the contributions of the initial weights and the weight mask, we next compared the three baselines to the full ticket. For most agents, training performance does not degrade substantially when the weights are permuted but the mask is kept intact (figure 2, middle column). This holds for both the value-estimation distillation of a DQN agent and the policy distillation of a PPO agent. The traditional *random/re-init* baseline performs worse already for moderate levels of sparsity. These

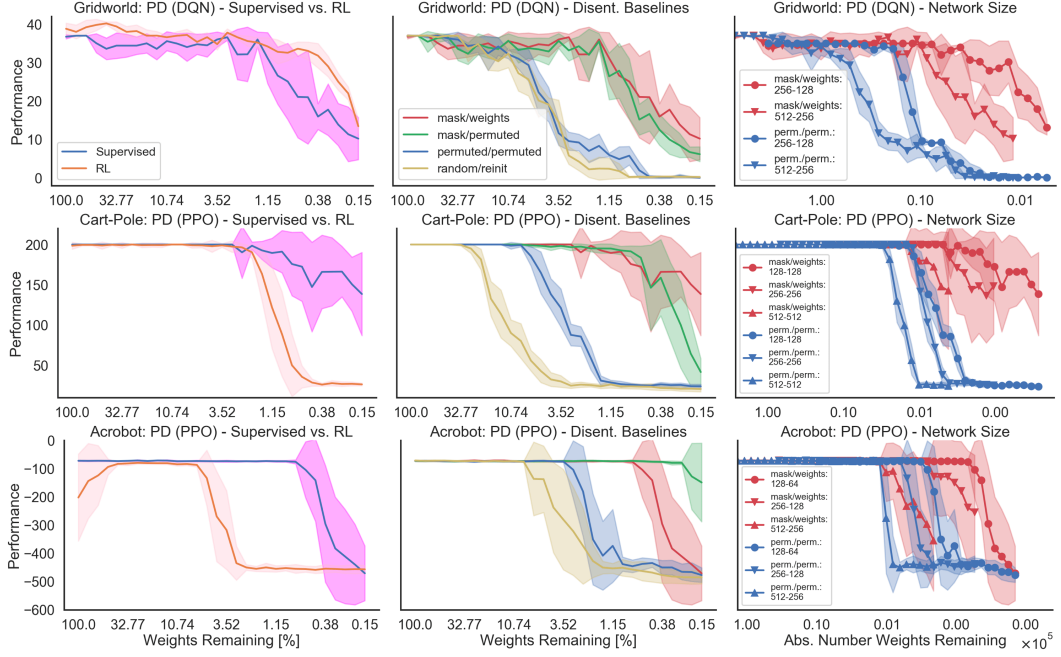


Figure 2: Lottery tickets in supervised policy distillation. **Left.** Comparing tickets in DRL and supervised policy distillation. Both training paradigms allow for similar levels of sparsity before the performance starts to degrade. **Middle.** Disentangling baselines for tickets in policy distillation. The gap between the ticket (*mask/weights*) and weight-permuted baseline (*mask/permuted*) is small, indicating a strong contribution of the mask to the overall effect. **Right.** The initial network size has no influence on relative performance of tickets and *permuted/permuted* baselines. Larger networks do not yield tickets that outperform those generated from smaller networks for a given absolute number of remaining weights. **Top.** Grid visual navigation task and DQN value estimate distillation. **Middle.** Cart-pole balancing task and PPO policy distillation. **Bottom.** Acrobot swing-up task and PPO policy distillation. Results are averaged over 5 independent runs on the GridMaze environment and 15 runs for both the Cart-Pole and Acrobot environments. We plot mean and one standard deviation.

insights emphasize the importance of strong and nuanced baselines to understand the contributions to the full lottery ticket effect in DRL.

The lottery ticket hypothesis suggests that using a larger original network size increases the number of sub-networks which may turn out to be winning tickets (Frankle and Carbin, 2019). To investigate this hypothesis for the case of policy distillation, we analyzed the effect of the initial network size on the lottery ticket effect (figure 2, right column). Against this initial intuition, we observe that smaller dense networks are capable of maintaining strong performance at higher levels of absolute sparsity as compared to their larger counterparts. Furthermore, the initial network size does not have a strong effect on the relative performance gap between the ticket configuration (*mask/weights*) and the baseline (*permuted/permuted*). We suspect that larger networks can not realize their combinatorial potential due to an unfavorable layer-wise pruning bias introduced by initialization schemes such as the Kaiming family (He et al., 2015). An imbalance between input size and hidden layer size can have strong impact on which weights are targeted by IMP. We further investigate this relationship in section 4.2.

To test the robustness of the lottery ticket phenomenon to different architectures and more challenging tasks, we repeat the previous baseline comparison distillation experiments in the more challenging MinAtar environments (see figure 3). We trained MLP- and CNN-based agents to distill experts' value estimators and using the same architecture and hyperparameters for all considered games (see SI). For MLP agents the mask consistently contributes most to the ticket. For CNN-based agents and selected games (Asterix and Space Invaders) the weight initialization contributes more.

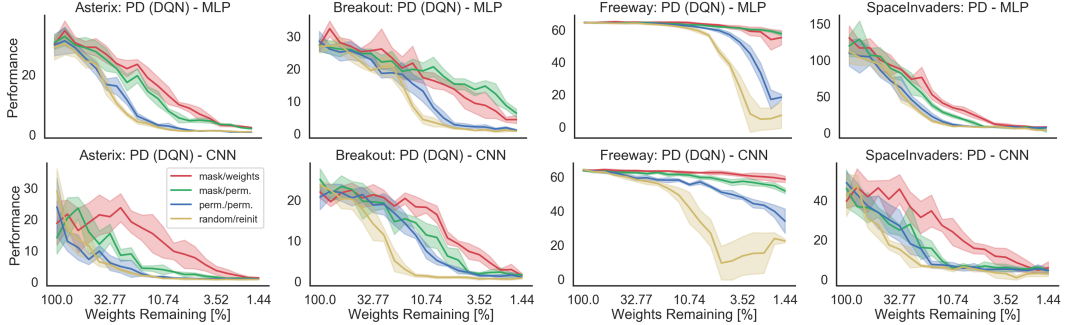


Figure 3: Lottery tickets in supervised policy distillation (MinAtar environments, Young and Tian, 2019). We find evidence for a strong contribution of the IMP-identified mask to the overall ticket effect. The qualitative baseline comparison generalizes from MLP- to CNN-based agents. **Top.** Disentangling ticket baselines for MLP-based value function estimators across four MinAtar games. **Bottom.** Disentangling ticket baselines for CNN-based value function estimators across four MinAtar games. The results are averaged over 5 independent runs for all MinAtar environments. We plot mean and one standard deviation.

3.2 Disentangling Ticket Contributions in Deep Reinforcement Learning

The observations that ticket information is mostly carried by the mask rather than the initial weights and that larger networks allow sparser tickets carry over to the full DRL setups (figures 4 and 5). A key difference between PPO and DQN methods lies in how the network’s weights influence the agents’ exploratory behavior: In PPO, exploratory actions are sampled from the stochastic policy. In DQN, actions are often chosen by an ϵ -greedy policy, in which exploratory actions do not depend on the network output. Therefore, one would expect that PPO agents cannot be pruned as aggressively, because this could impair exploration behavior. Contrary to this hypothesis, we find that for the cart-pole task, PPO agents train to strong performance at high levels of sparsity, while DQN performance already decreases for already moderate levels of sparsity (figure 4). For the visual navigation task we find the opposite behavior. Therefore, whether a network can be strongly pruned depends not on the choice of the algorithm alone, but rather on the combination of algorithm and task. This suggests that the degree to which winning tickets exist and their strength depends also on how well the optimization procedure is tailored to the underlying problem: DQN was developed for visual tasks, PPO for low-dimensional control.

Providing more empirical evidence for our previous claims, we find that for most MLP and CNN agents trained on the MinAtar games the ticket effect is explained by the IMP-discovered mask (see figure 5). Strengthening an observation in Yu et al. (2019), we observe that the performance deteriorates at different levels of network sparsity depending on the considered game. Freeway agents keep performing well even for high levels of sparsity, while agents trained on Breakout and Space Invaders continually get worse as the sparsity level increases. In general we find that the qualitative results obtained for MLP agents generalize well to CNN-based agents. The only major difference is that unlike the Asterix CNN agent, the MLP agent improves their performance at moderate levels of sparsity. In summary, we provide evidence for the strong contribution of the mask to the lottery ticket effect in DRL (both on-policy and off-policy algorithms). The results generalize between different architectures indicating that the strength of the overall lottery ticket effect is mainly dictated by the combination of the task-specification of the environment and the DRL algorithm.

4 Minimally Task-Sufficient Representations via IMP

The previous results point towards an interplay between the discovered mask and the environment specification. To better understand this phenomenon and the resulting inductive biases, we analyzed the sparsified weight matrices. The next section sets out to answer the following questions: **1)** What do the masked MLP-based agents observe? The derived mask can be thought of as a pair of goggles which guide the processing of state information. **2)** Can we transfer the input layer mask and re-use it

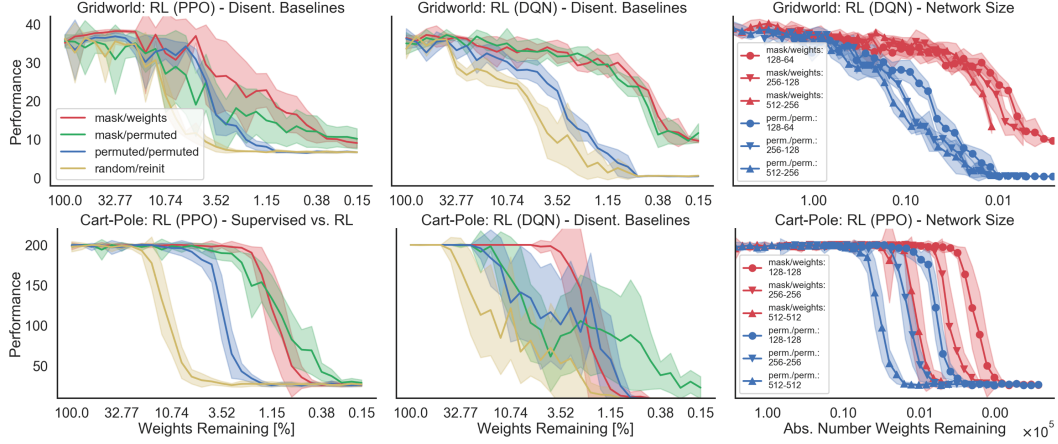


Figure 4: Tickets in on- and off-policy deep reinforcement learning. **Left.** Disentangling baselines for tickets in on-policy DRL (PPO) for a visual navigation (top) and cart-pole balancing task (bottom). **Middle.** Disentangling baselines for tickets in off-policy DRL (DQN). For both DQN on the visual navigation task and PPO on the cart-pole task most of the observed ticket effect can be attributed to the contribution of the mask and not the weight initialization. **Right.** Initial network size comparison for tickets in on- and off-policy DRL. Again, larger initial network size does not lead to more performant tickets. The results are averaged over 5 independent runs on the GridMaze environment and 15 independent runs on the Cart-Pole environment. We plot mean and one standard deviation.

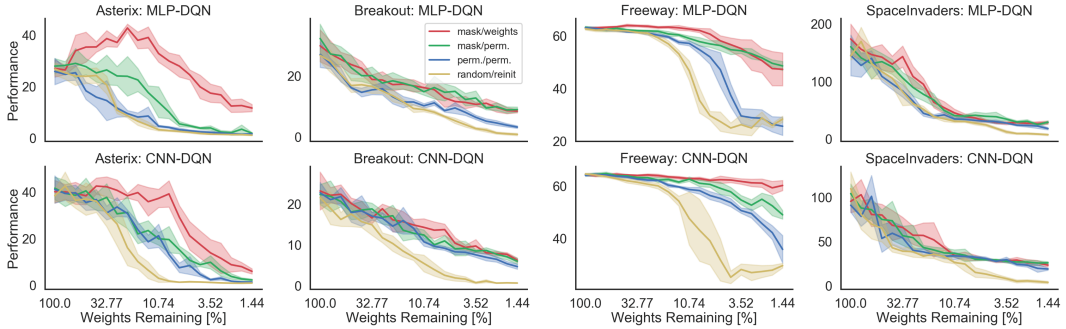


Figure 5: Tickets in off-policy deep reinforcement learning (MinAtar environments, Young and Tian, 2019). We find evidence for a strong contribution of the IMP-identified mask to the overall ticket effect. The qualitative baseline comparison generalizes from MLP- to CNN-based agents. **Top.** Disentangling ticket baselines for MLP-based value function estimators across four MinAtar games. **Bottom.** Disentangling ticket baselines for CNN-based value function estimators across four MinAtar games. The results are averaged over 5 independent runs for all MinAtar environments. We plot mean and one standard deviation.

as an inductive bias for otherwise dense agents? 3) How much influence do weight initialization and input dimensionality have on the discovered input layer mask?

4.1 Minimal Task Representations in High-Dimensional Visual Tasks

In the visual navigation experiments, the pruning primarily affects the input layer (figure 6, top right column). When visualizing the cumulative absolute weights of the input layer for an IMP-derived DQN agent, we find that IMP deletes entire dimensions from the observation vector (figure 6, left column) by removing all connections between those dimensions and the first hidden layer. These eliminated input dimensions are not task-relevant. A fully-connected network trained on the remaining dimensions learns the task as quickly as when trained on the complete set of input dimensions (figure 6, bottom right column). Hence, the IMP-derived mask provides a compressed representation of a

high-dimensional observation space, enabling successful training even at high levels of sparsity. This result extends to masked input layers of MLP-agents trained on the MinAtar environments (figure 7 and SI). For the Freeway task we find that the IMP mask encodes the notion of velocity of moving cars. The channel encoding the slowest moving car is pruned the most, maintaining only the pixels needed to react in time. The same principle applies to the enemy bullet channel in the SpaceInvaders task. The agent only needs to know about a potential collision at the next time step in order to avoid being hit. Therefore, IMP prunes all information about the enemy bullet that is more than one step away from the agent. For all visualized MinAtar tasks, only the actionable row/column of the agent channel is preserved. In Breakout, additionally the first row of the ball and trail channel is pruned since the game terminates once the ball or trail reach it. There is no action-relevant information encoded and it can be discarded. In summary, we find that IMP-derived input layer mask provides a visually interpretable and physically meaningful compression of the observation space.

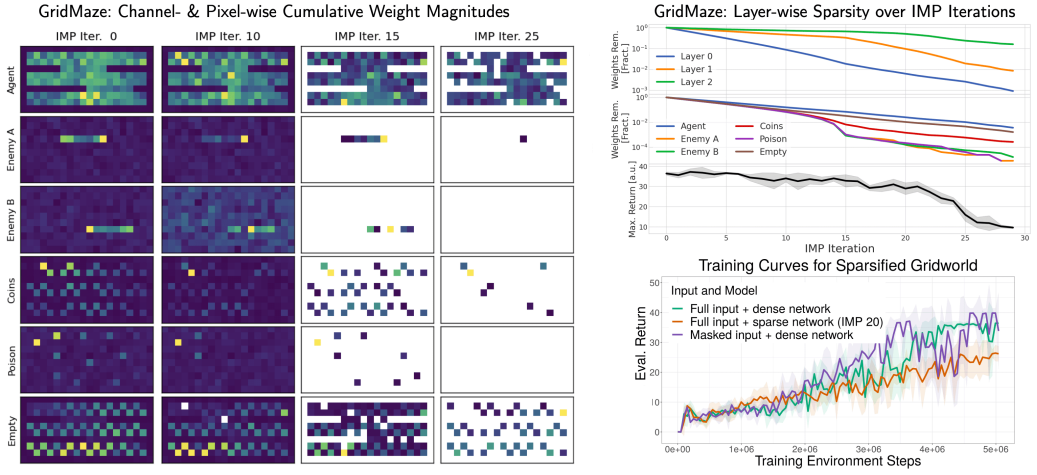


Figure 6: IMP eliminates task-irrelevant observation dimensions for a high-dimensional visual navigation task ($o_t \in \mathbb{R}^{6 \times 10 \times 20}$). **Left.** Channel-/pixel-wise cumulative weight magnitudes. IMP successively prunes redundant input pixels which are not necessary to solve the navigation task. All of the pruned enemy channel pixels encode locations which the patrolling enemy cannot access. **Right, Top.** Pruning affects the layers and object channels differentially. The input layer is pruned most strongly, while the agent channel is pruned the least. **Right, Bottom.** The input layer pruning mask (at moderate sparsity levels) can be used as an inductive bias for training a dense network.

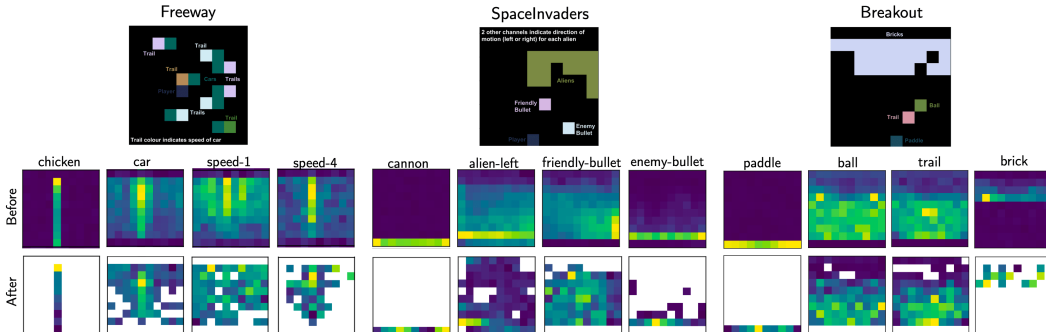


Figure 7: IMP eliminates task-irrelevant observation dimensions for a selection of MinAtar environments (Young and Tian, 2019). The environment depicting figures were adapted from Young and Tian (2019). **Left.** Freeway. IMP provides an inductive bias by differentially pruning object channels with different velocities (e.g. car speeds). **Middle.** SpaceInvaders. IMP only preserves pixels of enemy objects which encode actionable proximity information (e.g. bullets being close to the agent). **Right.** Breakout. IMP discards pixels which only change when it is too late to act (e.g. when the ball has left the display and the episode terminates).

4.2 Minimal Representations in Low-Dimensional Control Tasks and the Issue of Initialization Scales

The cart-pole and acrobot swing-up task, on the other hand, are low-dimensional control tasks. At first sight, they do not contain obviously uninformative input dimensions that lend themselves to be pruned. We would expect the cumulative weight strength of each input dimension to decrease at equal speed over the course of iterative pruning. Contrary to this initial intuition, we find that IMP still aggressively prunes core dimensions while yielding trainable agents (figure 8). For the cart-pole task, the cart position and its velocity are pruned. The pole’s angle and angular velocity sufficiently describe the required information needed to solve the task. This could be a consequence of the invariance of Newton’s laws to the choice of the inertial frame of reference. For the acrobot task the agent has to swing-up a two-link pendulum to cross a line as fast as possible. For this task IMP eliminates all sine and cosine transformations of the rotational angles of the links (figure 8, middle row, right column). Since the swing-up can be achieved by coordinating and increasing the angular velocities of the two links, only these two dimensions have to be preserved from pruning. This demonstrates that IMP can yield fundamental insights into what physical information is sufficient to solve a task.

During our analysis we discovered that the core dimension discovery of IMP crucially depends on the initialization of the input layer weights. Popular weight initialization heuristics such as the Kaiming family (He et al., 2015) aim to preserve activation magnitudes across network layers. As a result, layers that receive high-dimensional input are initialized at lower values and are therefore prone to more aggressive pruning by IMP. This bias does not occur for Xavier initializations (Glorot and Bengio, 2010, figure 8, top rows, right column). Furthermore, we experimented with different approaches to combat this initialization bias. We find that downscaling the Kaiming initialization of the input layer by a factor of ten lead to a robust discovery after few IMP iterations (figure 8, top rows, middle column). While smaller rescaling factors lead to a slower separation of dimensions, larger factors result in overly aggressive pruning of the input layer. In summary, we have shown that the input layer initialization can shape the resulting lottery ticket mask and provide a first initialization heuristic promoting efficient minimal task representation discovery.

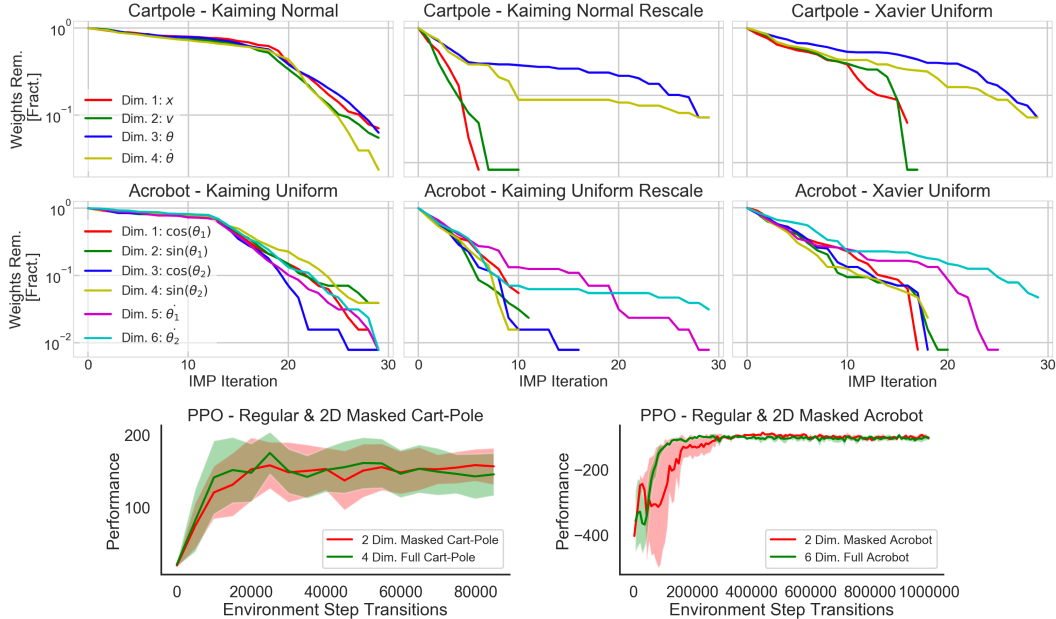


Figure 8: IMP eliminates task-irrelevant observation dimensions for a low-dimensional control tasks. **Top.** IMP identifies that the cart-pole task can be solved with only two dimensions: The pole angle and angular velocity. **Middle.** IMP identifies that the acrobot task can be solved with only two dimensions: The angular velocities of the two pendulum links. **Bottom.** Agents can successfully be trained on the subset of IMP-derived dimensions alone.

5 Conclusion

This work has investigated the mechanisms underlying the lottery ticket effect in DRL. We find that it can be mainly attributed to the identified mask as compared to the corresponding weight initialization. While this observation appears robust, it varies to some extent across learning paradigms, algorithms, architectures and qualitatively different tasks. Future work will need to untangle for which tasks, DRL objectives and optimization algorithms the initialization of the weight values contributes to the ticket effect. We have shown that the mask compresses the input representation by removing task-irrelevant information. Whether this interpretation also holds for intermediate and higher layer masks is hard to assess and remains an open question. We believe that there are many opportunities to modify the original IMP procedure to simplify the discovery of minimal representations. For example, pruning entire units of intermediate layers may improve the interpretability of hidden representations. Finally, we found that the pruning process is sensitive to the layer-specific scale of the weight initialization by heuristically re-scaling the weights in different layers. In future work we want to investigate these layer-specific effects, e.g., by studying layer-specific pruning ratios, normalization schemes and baseline analyses, in the hope of identifying sparser, more efficient and interpretable winning tickets not only in DRL.

References

BELLEMARE, M. G., Y. NADDAF, J. VENESS, AND M. BOWLING (2013): “The arcade learning environment: An evaluation platform for general agents,” *Journal of Artificial Intelligence Research*, 47, 253–279.

BROCKMAN, G., V. CHEUNG, L. PETTERSSON, J. SCHNEIDER, J. SCHULMAN, J. TANG, AND W. ZAREMBA (2016): “Openai gym,” *arXiv preprint arXiv:1606.01540*.

CHEN, T., J. FRANKLE, S. CHANG, S. LIU, Y. ZHANG, M. CARBIN, AND Z. WANG (2020a): “The Lottery Tickets Hypothesis for Supervised and Self-supervised Pre-training in Computer Vision Models,” *arXiv preprint arXiv:2012.06908*.

CHEN, T., J. FRANKLE, S. CHANG, S. LIU, Y. ZHANG, Z. WANG, AND M. CARBIN (2020b): “The lottery ticket hypothesis for pre-trained bert networks,” *arXiv preprint arXiv:2007.12223*.

CHEN, T., Z. ZHANG, S. LIU, S. CHANG, AND Z. WANG (2021): “Long live the lottery: The existence of winning tickets in lifelong learning,” in *International Conference on Learning Representations, 2021a*. URL <https://openreview.net/forum>.

DESAI, S., H. ZHAN, AND A. ALY (2019): “Evaluating lottery tickets under distributional shifts,” *arXiv preprint arXiv:1910.12708*.

FRANKLE, J. AND M. CARBIN (2019): “The lottery ticket hypothesis: Finding sparse, trainable neural networks,” *arXiv preprint arXiv:1803.03635*.

FRANKLE, J., G. K. DZIUGAITE, D. M. ROY, AND M. CARBIN (2019): “Stabilizing the lottery ticket hypothesis,” *arXiv preprint arXiv:1903.01611*.

——— (2020a): “Linear Mode Connectivity and the Lottery Ticket Hypothesis,” *arXiv preprint arXiv:1912.05671*.

FRANKLE, J., D. J. SCHWAB, AND A. S. MORCOS (2020b): “The Early Phase of Neural Network Training,” *arXiv preprint arXiv:2002.10365*.

GIRISH, S., S. R. MAIYA, K. GUPTA, H. CHEN, L. DAVIS, AND A. SHRIVASTAVA (2020): “The Lottery Ticket Hypothesis for Object Recognition,” *arXiv preprint arXiv:2012.04643*.

GLOROT, X. AND Y. BENGIO (2010): “Understanding the difficulty of training deep feedforward neural networks,” in *Proceedings of the thirteenth international conference on artificial intelligence and statistics*, JMLR Workshop and Conference Proceedings, 249–256.

HAN, S., J. POOL, J. TRAN, AND W. J. DALLY (2015): “Learning both weights and connections for efficient neural networks,” *arXiv preprint arXiv:1506.02626*.

HARRIS, C. R., K. J. MILLMAN, S. J. VAN DER WALT, R. GOMMERS, P. VIRTANEN, D. COURNAPEAU, E. WIESER, J. TAYLOR, S. BERG, N. J. SMITH, ET AL. (2020): “Array programming with NumPy,” *Nature*, 585, 357–362.

HASTIE, T., R. TIBSHIRANI, AND M. WAINWRIGHT (2019): *Statistical learning with sparsity: the lasso and generalizations*, Chapman and Hall/CRC.

HE, K., X. ZHANG, S. REN, AND J. SUN (2015): “Delving deep into rectifiers: Surpassing human-level performance on imagenet classification,” in *Proceedings of the IEEE international conference on computer vision*, 1026–1034.

HUNTER, J. D. (2007): “Matplotlib: A 2D graphics environment,” *IEEE Annals of the History of Computing*, 9, 90–95.

MEHTA, R. (2019): “Sparse transfer learning via winning lottery tickets,” *arXiv preprint arXiv:1905.07785*.

MNIH, V., K. KAVUKCUOGLU, D. SILVER, A. A. RUSU, J. VENESS, M. G. BELLEMARE, A. GRAVES, M. RIEDMILLER, A. K. FIDJELAND, G. OSTROVSKI, ET AL. (2015): “Human-level control through deep reinforcement learning,” *nature*, 518, 529–533.

MORCOS, A., H. YU, M. PAGANINI, AND Y. TIAN (2019): “One ticket to win them all: generalizing lottery ticket initializations across datasets and optimizers,” in *Advances in Neural Information Processing Systems*, 4933–4943.

OBANDO-CERON, J. S. AND P. S. CASTRO (2020): “Revisiting Rainbow: Promoting more insightful and inclusive deep reinforcement learning research,” *arXiv preprint arXiv:2011.14826*.

PASZKE, A., S. GROSS, S. CHINTALA, G. CHANAN, E. YANG, Z. DEVITO, Z. LIN, A. DESMAISON, L. ANTIGA, AND A. LERER (2017): “Automatic differentiation in pytorch,” .

RUSU, A. A., S. G. COLMENAREJO, C. GULCEHRE, G. DESJARDINS, J. KIRKPATRICK, R. PASCANU, V. MNIH, K. KAVUKCUOGLU, AND R. HADSELL (2015): “Policy distillation,” *arXiv preprint arXiv:1511.06295*.

SCHAUL, T., J. QUAN, I. ANTONOGLOU, AND D. SILVER (2015): “Prioritized experience replay,” *arXiv preprint arXiv:1511.05952*.

SCHMITT, S., J. J. HUDSON, A. ZIDEK, S. OSINDERO, C. DOERSCH, W. M. CZARNECKI, J. Z. LEIBO, H. KUTTLER, A. ZISSERMAN, K. SIMONYAN, ET AL. (2018): “Kickstarting deep reinforcement learning,” *arXiv preprint arXiv:1803.03835*.

SCHULMAN, J., F. WOLSKI, P. DHARIWAL, A. RADFORD, AND O. KLIMOV (2017): “Proximal policy optimization algorithms,” *arXiv preprint arXiv:1707.06347*.

STOOKE, A. AND P. ABBEEL (2019): “rlpyt: A research code base for deep reinforcement learning in pytorch,” *arXiv preprint arXiv:1909.01500*.

VAN HASSELT, H., A. GUEZ, AND D. SILVER (2016): “Deep reinforcement learning with double q-learning,” in *Proceedings of the AAAI Conference on Artificial Intelligence*, vol. 30.

WASKOM, M. L. (2021): “Seaborn: statistical data visualization,” *Journal of Open Source Software*, 6, 3021.

YOUNG, K. AND T. TIAN (2019): “Minatar: An atari-inspired testbed for thorough and reproducible reinforcement learning experiments,” *arXiv preprint arXiv:1903.03176*.

YU, H., S. EDUNOV, Y. TIAN, AND A. S. MORCOS (2019): “Playing the lottery with rewards and multiple languages: lottery tickets in RL and NLP,” *arXiv preprint arXiv:1906.02768*.

Supplementary Information

A MazeGrid Environment

The MazeGrid is a visual navigation task: The agent navigates a grid environment, which is ten pixels high and twenty pixels wide. Each location holds a single unique object. There are six types of objects: empty background (black), walls (grey), the agent (cyan), two moving enemies (magenta and green), as well as 42 coins (yellow) and twelve poisons (brown) (visualized in figure 1, bottom row, left column). The layout of the game is the same in every episode. The agent can walk in four directions (up, down, left, right). The enemies patrol horizontally inside the gaps in the wall. A full game in motion can be watched in the project repository, which will be released after publication. A game terminates after 200 timesteps, or if the agent collects (walks over) all coins, or if the agent is in the same location as an enemy. Each collected coin yields a reward of plus one, each collected poison yields minus one, presented immediately to the agent. To ensure our results do not depend on the specific encoding of the environment, we compared three different representation of the MazeGrid environment (section C.2):

- The **object-map** encoding consists of separate one-hot maps for each type of object. Empty space is encoded explicitly by a separate map, walls however do not have their own map and are only implicitly represented by the lack of any other object. The representation thus contains six maps, ten by twenty pixels each for a total of 1200 binary values for each state.
- The **RGB** encoding consists of the canonical three color channels for each location, resulting in 600 integer values in range $[0, 255]$. Losing information due to occlusion is not an issue in this environment since any location can only hold a single object at a time.
- The **entangled** encoding is derived from the object-map encoding by flattening all values into a vector and multiplying it with a pseudo-random 1200 by 1200 matrix. The matrix's values are sampled independently from $\mathcal{U}(-1, 1)$. The matrix remains constant across all IMP iterations, every seed has its own matrix.

All experiments in the main text were conducted on the object-map environment. Figure 10 provides a comprehensive overview over the baselines to demonstrate that tickets do rely on one specific encoding. The importance of the mask is even further highlighted by our results on RGB specifically.

B Hyperparameter Settings for Reproduction

All simulations were implemented in Python using the rlpyt DRL training package (Stooke and Abbeel, 2019, MIT License) and PyTorch pruning utilities (Paszke et al., 2017). The environments were implemented by the OpenAI gym (Brockman et al., 2016, MIT License) and MinAtar (Young and Tian, 2019, GPL-3.0 License) packages. Furthermore, all visualizations were done using Matplotlib (Hunter, 2007) and Seaborn (Waskom, 2021, BSD-3-Clause License). Finally, the numerical analysis was supported by NumPy (Harris et al., 2020, BSD-3-Clause License). We will release the code after the publication of the paper. The simulations were conducted on a CPU cluster and no GPUs were used. Each individual IMP run required between 8 (cart-pole and acrobot) and 20 cores (MazeGrid and MinAtar environments). Depending on the setting, a set of 20 to 30 iterations lasts between 0.5 and 5 days of training time.

B.1 GridMaze - Policy Distillation

Parameter	Value
Student Network Size	128,64 units and 256,128 units
Teacher Network Size	64,32 units and 128,64 units
Learning Rate	0.0005
Training Environment Steps	2.000.000
Independent Seeds	5
Distillation Loss	MSE of expert-student values

Table 2: Hyperparameters for the **policy distillation** learning algorithm on **GridMaze**. Results reported in figure 2, top row.

B.2 GridMaze - Deep-Q-Networks and PPO

Parameter	Value	Parameter	Value
Optimizer	Adam	Replay Buffer Size	100.000
Learning Rate	0.0005	Replay Buffer α	0.6
Temporal Discount Factor	0.99	Replay Buffer β (init.)	0.4
Batch Size	256	Replay Buffer β (final)	1
Huber Loss δ	1.0	Data Replay Ratio	4
Clip Grad. Norm	10	Training Environment Steps	5.000.00
Independent Seeds	5		

Table 3: Hyperparameters for the **DQN** learning algorithm on **GridMaze**. Results reported in figure 4, top row, middle column.

Parameter	Value	Parameter	Value
Optimizer	Adam	Value Loss Coeff.	1
Learning Rate	0.0001	Entropy Loss Coeff.	0.01
Temporal Discount Factor	0.99	Likelihood Ratio Clip	0.1
Training Environment Steps	10.000.00	Independent Seeds	5

Table 4: Hyperparameters for the **PPO** learning algorithm on **GridMaze**. Results reported in figure 4, top row, left column.

B.3 Cart-Pole - Policy Distillation

Parameter	Value
Student Network Size	128,128 units and 256,256 units
Teacher Network Size	64,64 units and 128,128 units
Learning Rate	0.001
Training Environment Steps	10.000
Independent Seeds	15
Distillation Loss	Cross-entropy expert-student policies

Table 5: Hyperparameters for the **policy distillation** learning algorithm on **Cart-Pole**. Results reported in figure 2, bottom row.

B.4 Cart-Pole - Deep-Q-Networks and PPO

Parameter	Value	Parameter	Value
Optimizer	Adam	Clip Grad. Norm	10
Learning Rate	0.001	Replay Buffer Size	20.000
N-Step Returns	3	Replay Buffer α	0.6
Temporal Discount Factor	0.9	Replay Buffer β (init.)	0.4
Batch Size	128	Replay Buffer β (final)	1
Huber Loss δ	1.0	Data Replay Ratio	4
Training Environment Steps	80.000	Independent Seeds	15

Table 6: Hyperparameters for the **DQN** learning algorithm on **Cart-Pole**. Results reported in figure 4, bottom row, middle column.

Parameter	Value	Parameter	Value
Optimizer	Adam	Value Loss Coeff.	0.5
Learning Rate	0.0005	Entropy Loss Coeff.	0.001
Temporal Discount Factor	0.99	Likelihood Ratio Clip	0.2
Training Environment Steps	80.000	Independent Seeds	15

Table 7: Hyperparameters for the **PPO** learning algorithm on **Cart-Pole**. Results reported in figure 4, bottom row, left column.

B.5 Acrobot - Policy Distillation

Parameter	Value
Student Network Size	128,64 and 256,128 and 512,256 units
Teacher Network Size	128,64 units
Learning Rate	0.0005
Training Environment Steps	200.000
Independent Seeds	15
Distillation Loss	Cross-entropy expert-student policies

Table 8: Hyperparameters for the **policy distillation** learning algorithm on **Acrobot**. Results reported in figure 2, bottom row.

B.6 MinAtar - Policy Distillation for MLP/CNN Agents

Parameter	Value
Student Network Size	1024,512 units (MLP) and Conv2D-16x3, 128-64 (CNN)
Teacher Network Size	512,256 units (MLP) and Conv2D-16x3, 128-64 (CNN)
Learning Rate	0.0005
Training Environment Steps	10.000.000 (MLP) and 5.000.000 (CNN)
Independent Seeds	5
Distillation Loss	MSE of expert-student values

Table 9: Hyperparameters for the **policy distillation** learning algorithm on **MinAtar** environments. Results reported in figure 3.

B.7 MinAtar - Deep-Q-Networks for MLP/CNN Agents

Parameter	Value	Parameter	Value
Optimizer	Adam	Replay Buffer Size	100.000
Learning Rate	0.00025	Replay Buffer α	0.6
Temporal Discount Factor	0.99	Replay Buffer β (init.)	0.4
Batch Size	256	Replay Buffer β (final)	1
Huber Loss δ	1.0	Data Replay Ratio	4
Clip Grad. Norm	10	Training Environment Steps	15.000.00
Independent Seeds	5		

Table 10: Hyperparameters for the **DQN** learning algorithm on **MinAtar** environments. Results reported in figure 5.

C Additional Results

C.1 Performance of Different Training Paradigms on Cart-Pole and GridMaze

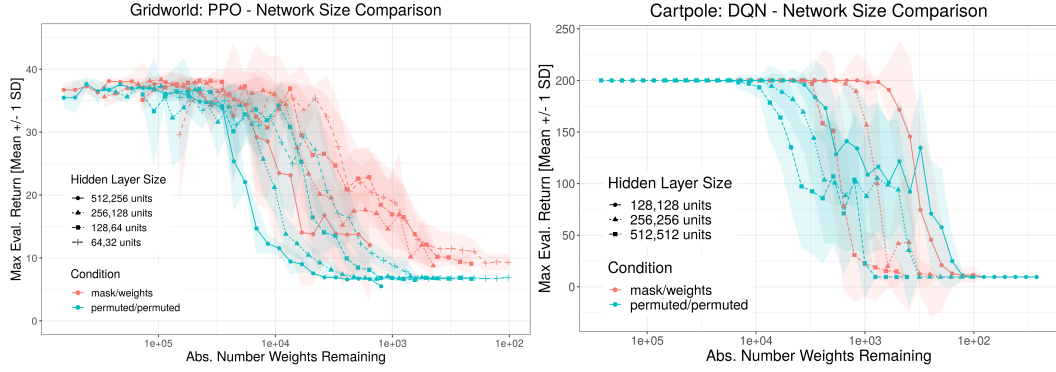


Figure 9: In the main text, agents were trained on GridMaze using the DQN algorithm and on cart-pole using PPO. Here, we report the performance of PPO-trained agents on the GridMaze task (left) and of DQN-trained agents on the cart-pole task (right) for different network sizes.

C.2 The Effect of Different Representations on Lottery Tickets in DRL

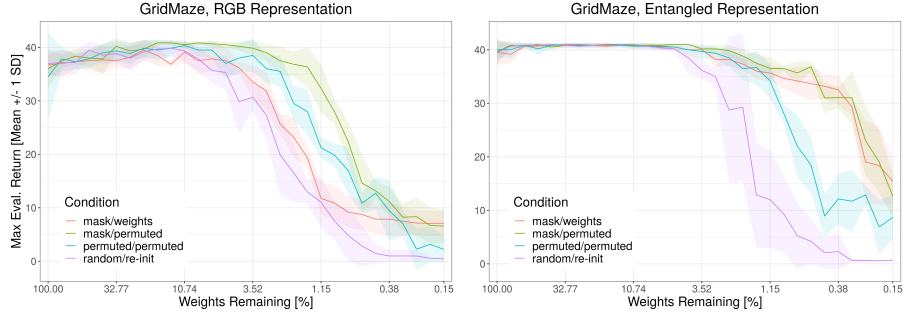


Figure 10: Performance of agents trained on an RGB-encoded GridMaze task (left) and on a randomly projected, entangled representation (right). The derived mask robustly contributes most to the ticket.

C.3 The Effect of Regularization and Late Rewinding on Lottery Tickets in DRL

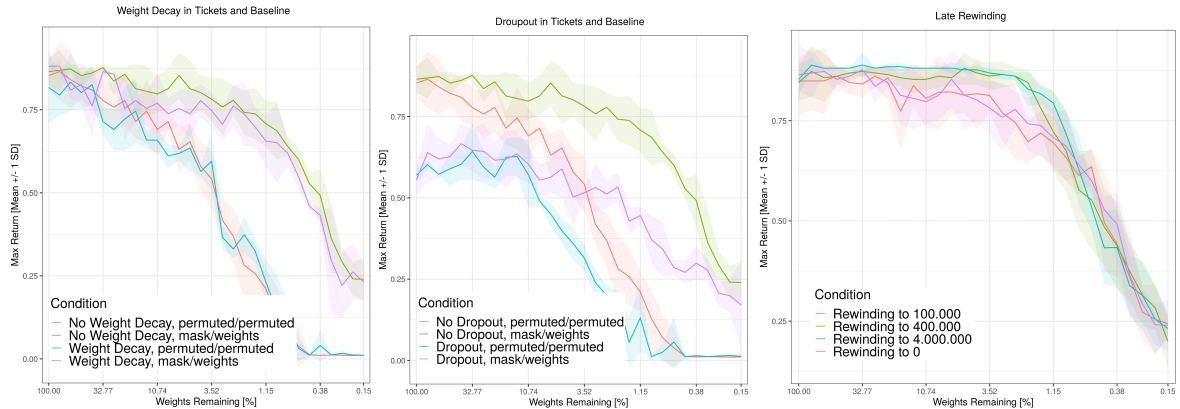


Figure 11: **Left.** Lottery ticket plot with and without L2 weight decay ($\lambda = 0.1$). Using weight decay does not impair the ticket phenomenon for a DQN agent. **Middle.** Lottery ticket plot with and without dropout in all layers ($p = 0.1$). Dropout deteriorates overall performance at all levels of sparsity, but does not impair the ticket effect for a DQN agent. **Right.** Late rewinding (Frankle et al., 2019) to different stages of training (0, 100k, 400k, 4000k environment steps).